Pergamon

Int. J. Heat Mass Transfer. Vol. 38, No. 10, pp. 1823–1830, 1995

0017-9310/95 $9.50+0.00

0017-9310(94)00307-6

Forced convection mass/heat transfer coefficient at the surface of the rotor of the sucking and forcing regenerative exchanger

B. BIENIASZ and J. WILK

Thermodynamics and Aircraft Engines Department, Rzeszów University of Technology, ul.W.Pola 2, 35-959 Rzeszów, Poland

(*Received* 24 *January* 1994 *and in final form* 7 *September* 1994)

Abstract—Experimental investigations of mean mass/heat transfer coefficients at the surface of two different curved short ducts of rotors of the sucking and forcing regenerative heat exchanger were made for forced laminar flow in static conditions. An electrolytic technique was employed. The results for two types of ducts are presented finally by correlations for j_M Chilton–Colburn coefficient vs Reynolds number. The results for one of the ducts are consistent with the previous results of the author for the inner surface and developed flow in a straight annular duct with similar L/D_h.

INTRODUCTION

For the purpose of ventilation with simultaneous heat regeneration, the sucking and forcing regenerative heat exchanger (SFE) may be applied [1, 2] in swimming pools, stores, classrooms, auditoriums, workshops, restaurants, waiting-rooms, paint shops, offices, vehicles, etc. A main part of the exchanger, i.e. rotor 1 (see Fig. 1), made as a capillary-porous cylinder, is driven by a small electric motor at a relatively high angular velocity of a few thousand revolutions per minute, which causes the suction and force process to occur. The simultaneous processes of heat, mass and momentum transfer between streams take place in the exchanger, yet heat transfer among them prevails. The internal suction volume of the rotor is divided into two volumes by an immovable partition 2. Warm, used up air enters the volume 3, flows through the ducts of the rotor being cooled and leaves the exchanger by channel 4. Cold, fresh air enters the volume 5, gets warm passing through the rotor and is discharged to the atmosphere through the passage 6.

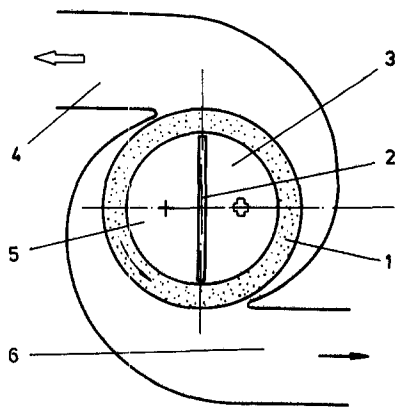

Fig. 1. Scheme of the sucking and forcing regenerative heat exchanger.

The chosen element of material of the rotor is heated and cooled alternately with the frequency of revolutions of the rotor. The heat transfer for the element is typically transient. A predominant component of energy balance of the SFE for one revolution of the rotor is the heat of convective heat transfer between the gas and the wall of a duct of the rotor. The heat is conducted inside the material and stored in it in the course of heating the rotor.

On entering a zone of cooling the rotor loses heat energy. So the thermal diffusivity of the material of the rotor should be rather high. Conditions for obtaining high heat power, per unit volume of the rotor, exchanged in this way, are also: high porosity of material of the rotor, which results in a high heat transfer surface area, and a high value of convective heat transfer coefficient. The latter has to be determined not only for energy balance calculations of the SFE. It also enables the local balance to be checked between the convectional heat power and the non-stationary heat energy power that can be stored in certain material of the rotor on a principle of heat capacity, during part of the period, at fixed angular velocity.

There are a few possible porous patterns of rotors resulting from technology. For two of them the mean, convective mass (heat) transfer coefficient was measured. The first pattern arose from the use of a round stamped corrugated sheet, the second from the above-mentioned sheets set alternately with plain ones in the rotor. As a result a structure consisting of short diffuser ducts with thin walls was obtained. It would be extremely difficult to tackle the problem exper-

NOMENCLATURE

A	surface area of the cathode
A_c	cross-section area of the duct
A_H	overall surface area of heat transfer of the rotor
c_{pg}	specific heat capacity of the gas at $p = \text{const}$
C_b	bulk concentration of ferricyanide ions
D	diffusivity of ferricyanide ions in the electrolyte
D_h	hydraulic diameter of the duct
F	Faraday constant $[96\,493 \times 10^3$ A s kmol$^{-1}]$
h	mean heat transfer coefficient
h_D	mean mass transfer coefficient
i	current density
I	current in the circuit
I_p	plateau current
j_H, j_M	mean Chilton–Colburn coefficient for heat and mass transfer, respectively
L	length of the duct
n	valence change of reacting ions
O_w	wetted circumference of reacting ions
R	radius of curvature of duct axis
Sc	Schmidt number, v/D
Sh	mean Sherwood number, $h_D D_h/D$
St_H	mean Stanton number for heat transfer, $h/(c_{pg}\rho_g w_g)$
St_M	mean Stanton number for mass transfer, h_D/w
U	voltage
w, w_g	mean velocity of electrolyte and gas, respectively
x	coordinate.

Greek symbols

δ	curvature ratio, D_h/R
μ	dynamic viscosity of electrolyte
v	kinematic viscosity of electrolyte
ρ, ρ_g	density of electrolyte and gas, respectively.

imentally using a thermal method. The only technique suitable in this case seemed to be an electrolytic one.

EXPERIMENTAL TECHNIQUE

Experiments were carried out by use of the well-known electrolytic technique [3, 4]. Nickel electrodes in aqueous solution of equimolar quantities of $K_3Fe(CN)_6$ and $K_4Fe(CN)_6$ in the presence of 1 M NaOH basic solution were applied. Nickel sheets of the rotor served as the cathode. An anode was located behind the cathode in the direction of flow of the electrolyte. The surface area of the anode was much greater than that of the cathode which enabled the controlled diffusion of ferricyanide ions at the cathode to be achieved. According to the conditions of the experiment one could omit mass-fluxes due to convection (with error about -0.5%) and due to migration on account of a small electrical potential gradient in the basic electrolyte in the direction perpendicular to the surface of the cathode. Thus current in a circuit resulted only from diffusion, and

$$h_D = I_p/(AFC_b). \quad (1)$$

The electrolyte was bubbled with nitrogen to avoid the influence of the presence of molecular oxygen on the results of the experiment. The temperature of the electrolyte was 25°C. Its essential physical properties were: $\rho = 1040$ kg m^{-3}, $\mu = 1.11 \times 10^{-3}$ kg m^{-1} s^{-1}, $D = 6.71 \times 10^{-10}$ m^2 s^{-1} which requires special comment.

The above values were calculated with the help of correlations stated experimentally, for temperatures of 18–30°C, by Hopkowicz and Pietrzyk [5] for the aqueous solution of 0.00333 N potassium ferricyanide and ferrocyanide in 1, 2 and 3 N sodium hydroxide. They directly measured ρ and μ with the help of a hydrostatic Mohr's balance and Hoppler's viscosimeter respectively. The diffusion coefficient was stated using a rotating disk electrode in an electrolysis cell. The Schmidt number was calculated from Sparrow and Gregg's correlation taking into consideration Newman's correction. For the electrolyte of a 1 M NaOH basic solution the following correlations were stated:

$$\rho = 1137.9 - 0.33T \text{ [kg m}^{-3}\text{]} \quad \text{(error of the correlation: } \pm 0.5\%) \quad (2)$$

$$\mu = 1.12 \times 10^{-6} \exp(2056.8/T) \text{ [kg m}^{-1}\text{ s}^{-1}\text{]} \quad (\pm 2.5\%) \quad (3)$$

$$D = 1.772 \times 10^{-6} \exp(-2348.9/T) \text{ [m}^2\text{ s}^{-1}\text{]} \quad (\pm 3.5\%) \quad (4)$$

in which $[T] = \text{K}$.

Lucas *et al.* [6] calculated the density of an aqueous solution of 0.01 N $K_4Fe(CN)_6$ in 1 N NaOH at 25°C assuming there is no volume change on mixing. Their result, which was checked using a hydrometer, was identical to that obtained by the help of equation (2). They also used a Cannon–Fenske viscometer to determine the viscosity, obtaining, for 25°C, the result $\mu = 1.109 \times 10^{-3}$ kg m^{-1} s^{-1} which differs from that calculated from equation (3) by 0.1%.

Bazan and Arvia [7] measured the viscosity of a

1.014 M solution of NaOH with centinormal quantities of potassium ferri- and ferrocyanide at 25°C and their result was identical to that of Lucas *et al.* They also stated that in a range of temperatures between 24 and 40°C Stokes–Einstein's equation

$$D\mu/T = (2.52 \pm 0.1) \times 10^{-15} \text{ [kg m s}^{-2} \text{ K}^{-1}\text{]} \ (\pm 4\%) \quad (5)$$

is valid, for ferricyanide ions, in an approximately 1 M sodium hydroxide basic electrolyte. They used the results of limiting current density measurements, under controlled convective diffusion at a rotating disk electrode, for calculating the diffusion coefficients by the help of Levich's equation. Setting in equation (5) the value of μ calculated by the help of equation (3) one gets, at 25°C, $D = 6.77 \times 10^{-10}$ m^2 s^{-1}, which differs from the value of D calculated on the basis of equation (4) by about 0.9%.

Eisenberg *et al.* [8] stated by direct measurement of the diffusion coefficient of $Fe(CN)_6^{3-}$ ions in an approximately 2 N NaOH basic solution, using McBain–Northrup type diaphragm cells, that the value of the constant in Stokes–Einstein's equation equals 2.5×10^{-15} kg m s^{-2} K^{-1}. They attained a reproducibility of diffusion coefficients of ferricyanide ions equal to $\pm 1.5\%$. Using the last constant and viscosity calculated according to equation (3) one gets, at 25°C, a value of the diffusion coefficient identical to that calculated with the help of equation (4).

RIG AND TEST SECTION

The experiments were carried out on the universal rig. Its electrolyte, nitrogen, water cooling and electrical measurement systems are presented in Fig. 2. It enabled polarization curves to be obtained automatically. Figure 3 presents a technical drawing of a test section, which was made mainly of PVC. The electrodes were machined from an electrolytical nickel sheet of thickness 0.2 mm. Flat anodes were glued to the flange. Two types of models of the rotor (cathodes) were combined from corrugated, Fig. 4, and flat, Fig. 5, nickel stamped elements of the rotor of the sucking and forcing heat exchanger. All elements had round cuts located at $2\pi/3$ rad from each other. There existed two patterns of corrugated elements, (a) and (b). The only difference between them was that the round cuts in pattern (b) were displaced by $\pi/60$ rad (3°) in comparison with pattern (a). The number of sheets was selected according to the need of attaining of maximum Reynolds number on appropriate level in ducts of the model as in ducts of real rotor and according to the electrolyte-flux available. Two models of the rotor were studied.

The type I model consisted of two corrugated sheets of pattern (a) and one corrugated sheet of pattern (b) between them. The position of elements was fixed by help of three pins which were adjusted to the round cuts in them. They were in contact with a plate, a right-sided flange and with one another at points of crests at the outside diameter. The distance between the plate and right-sided flange was adjusted with the help of the ring. The elements were covered with a thin (about 0.2 mm) layer of electrical insulation with the exception of one side of the inner sheet. This side was cautiously polished ultimately with diamond paste 1/0, a neutral tooth-paste containing chalk, and rinsed with distilled water. The inside element was welded at its outside edge to the 0.5 mm DIA electrically isolated nickel wire, which served as a connection of the cathode to the circuit. The axes of ducts obtained were curved (see Fig. 4). Cross-sections of the duct at inner and outside diameters and characteristic important data of the duct are depicted in Table 1. The ducts are curved diffusers communicating with themselves by contracting slits in a plane of points of contacts of sheet elements.

The type II model of the rotor consisted of three corrugated sheets of pattern (b) and two flat nickel stamped elements between them. They touched the plate and the flange, and together similarly as in the

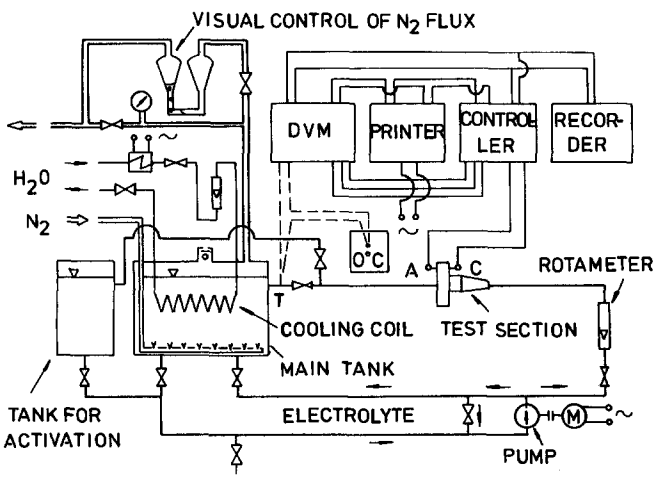

Fig. 2. The electrical measurement system.

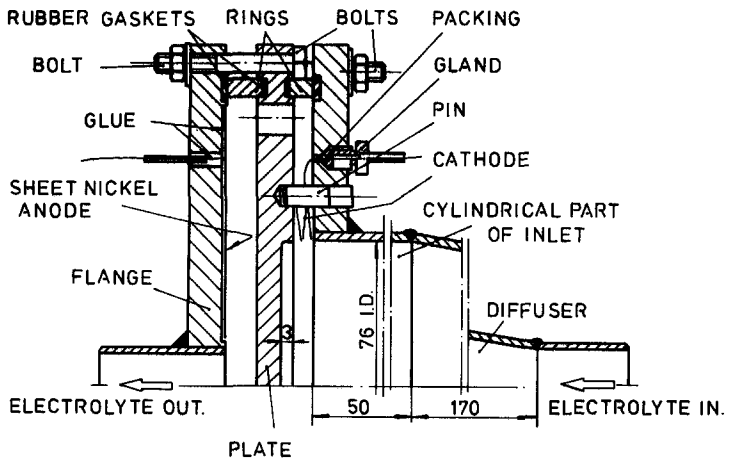

Fig. 3. Test section.

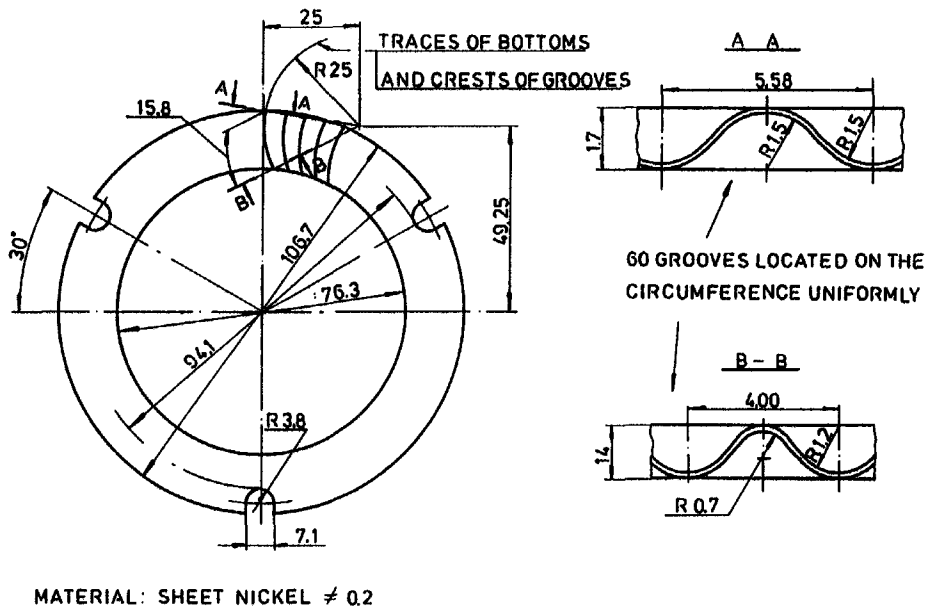

Fig. 4. Corrugated element of the rotor of the sucking and forcing heat exchanger.

case of the type I model. The middle corrugated element, electrically connected to the circuit, was the same as in the type I model. Its nickel surface and the opposite nickel surface of the adjacent flat element constituted the cathode. All other surfaces of elements were covered with electrical insulation as in the case of the type I model.

The curved, diffuser ducts resulting were of cross-section and had characteristic data as given in Table 1. Particularly notable is the much lower value of the arithmetic mean of the hydraulic diameter than for the type I ducts. The length of all the ducts is the length of the curve of the axis $L = 15.8$ mm. The value of the working surface of the cathode of the type I model was equal to 49.9 cm^2 and that of the type II model was equal to 91.8 cm^2 with relative error of $\pm 5\%$. The surface area of the corrugated element was calculated on the basis of geometric analysis of the element at its inner and outer diameters, and on the basis of the thickness of the sheet. The 'stamp-ratio', i.e. the ratio of the value of the surface area of the corrugated element to the value of the surface area of the flat one was equal to 1.19.

The temperature of the electrolyte was measured using a "Philips" integral chromel–alumel thermocouple placed between the test section and a tank. The maximum inaccuracy was ± 0.25 K.

EXPERIMENTAL METHOD

After installing the test section in the universal rig, activation of the cathode was carried out in a 5 N aqueous solution of NaOH at a current density $i = 20$

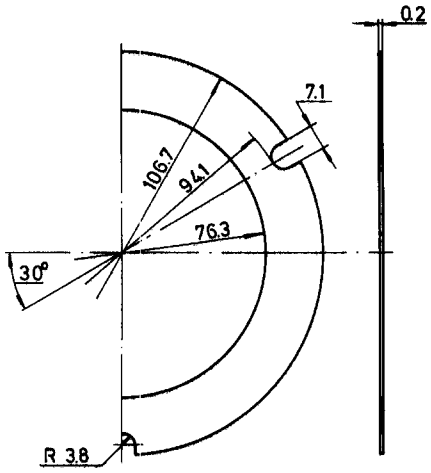

Fig. 5. Flat element of the rotor of the sucking and forcing heat exchanger.

mA cm^{-2} for 60 min. After changing over to the working electrolyte, trials were made to get the controlled diffusion at the cathode for the mean value of flux. The stage of trials and controlled diffusion treatment lasted 225 min in the case of a type I rotor and 165 min for a type II model. The next complete trial measurement was performed for an entire range of Reynolds numbers for 30 min. In the course of the next three days one measurement, for the same type of model of the rotor, for twelve different Reynolds numbers was carried out.

Polarization-curves, with *Re* as a parameter, were acquired automatically by applying, between anode and cathode, a stabilized voltage which changed by 0.1 V every few seconds. The values of current vs voltage were printed and registered graphically. The measurement for twelve Reynolds numbers lasted no more than 30 min. During it a sample of the electrolyte was taken and measurement of the concentration of ferricyanide ions, by iodometric titration, took place two or three times. The results were almost always identical. For the purpose of calculations an arithmetic mean was taken from all the titrations. The working ion concentration was considered as a constant owing to the relatively short time of measurement and the comparatively high concentration level.

After completing the trials, actual measurements were carried out during three succeeding days for a type I model of the rotor, for the same Reynolds numbers, and similarly for a type II model. One set of measurements for twelve Reynolds numbers was realized every day. The mass (heat) transfer coefficient was calculated as the arithmetic mean of the values

Table 1. Cross-section areas and hydraulic diameters of ducts of the rotor

Type of rotor	Place at	Sketch of the cross-section of the duct	Cross-section area of the duct A_c [mm^2]	Wetted circumference O_w [mm]	Hydraulic diameter $D_h = 4A_c/O_w$ [mm]	Mean hydraulic diameter $D_h = (D_{hI}+D_{hO})/2$ [mm]	Mean cross-section area $A_c = (A_{cI}+A_{cO})/2$ [mm^2]
I	i.d.	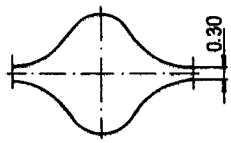	5.86	9.4	2.49		
						2.46 ±5%	7.00 ±5%
	o.d.	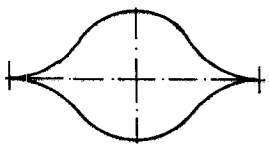	8.15	13.4	2.43		
II	i.d.	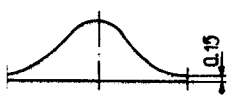	2.93	8.7	1.35		
						1.34 ±5%	3.50 ±5%
	o.d.		4.07	12.3	1.33		

obtained in three days of experiments for a given Reynolds number.

RESULTS OF MEASUREMENTS AND DISCUSSION

The Reynolds number was calculated on the basis of readings of the volumetric flux of the electrolyte on the rotameter, which had been calibrated beforehand by the use of an orifice plate. Taking into account maximum errors of reckoning of real volumetric flux of the electrolyte (±1.5%), mean cross-section area of the duct (±5%), mean velocity of electrolyte in the duct (±5.1%), mean hydraulic diameter of the duct (±5%), and coefficient of kinematic viscosity (±3%), the mean square error of the Reynolds number was calculated to be equal to ±7.4%. The mass transfer coefficient was calculated from equation (1). Ferricyanide ion concentration was measured with an accuracy of ±2%. The values of the concentration are given in Table 2.

Examples of polarization curves obtained are presented in Fig. 6. They testify to distinct controlled diffusion at the cathode in the entire range of Reynolds numbers. The inaccuracy of determining the plateau current was omitted. Taking additionally into account the relative error of the evaluation of surfaces of cathodes (±5%) one could calculate the mean square error of the mass transfer coefficient, which was equal to 5.4%. Having got the diffusivity of ferricyanide ions with an accuracy of ±5% one could calculate the Sherwood number with a mean square error ±8.9%.

The results of calculations of the mean value of the Sherwood number vs Reynolds number are depicted

Table 2. Values of concentration of ferricyanide ions in the electrolyte: $C_b \times 10^{-4}$ kmol m^{-3}

Number of measurements	Type I model of the rotor	Type II model of the rotor
1	17.6	9.0
2	15.6	8.2
3	14.4	6.6

in Fig. 7 as graphical correlations, for both types of models investigated. The error of correlation can be stated as being equal to 16.3%. The mean value of the Sherwood number for the duct of type I is much greater than that for the duct of type II. The mean ratio of them is equal to 1.83 in the interval of Reynolds numbers from 200 to 900.

The results of measurements of the mass transfer coefficient were also presented in the form of the Chilton–Colburn coefficient for mass transfer to permit the easy use of them for calculations of the heat transfer coefficient, at the surface of the duct, based on the Chilton–Colburn analogy. The mean value of the C–C coefficient for the whole surface was calculated thus:

$$j_M = St_M\, Sc^{2/3}. \tag{6}$$

The results are shown in Fig. 8. For particular Reynolds numbers points were marked on the basis of arithmetic means of $j_{M,i}$ from three independent measurements as mentioned above. Maximum deviations $(j_{M,i}-j_M)\times 100\%/j_M$ for the whole range of Reynolds numbers are contained in the interval from −4.0 to +3.7% for the type I model of the rotor and from −4.2 to +5.0% for the type II model. The

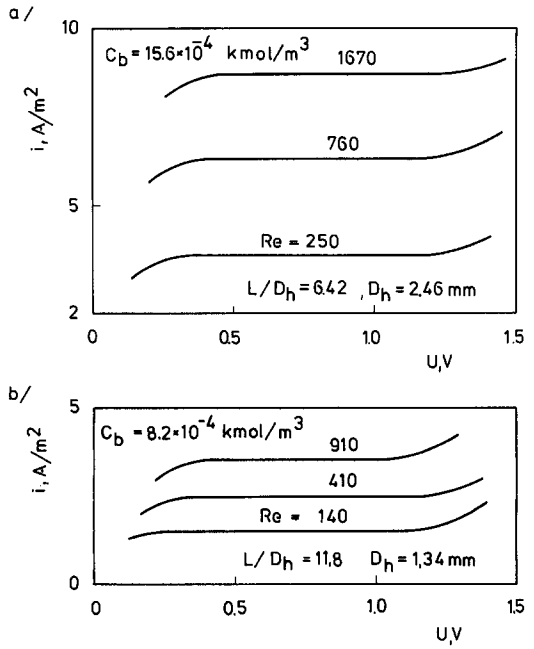

Fig. 6. Examples of polarization curves for ducts of: type I (a) and type II (b).

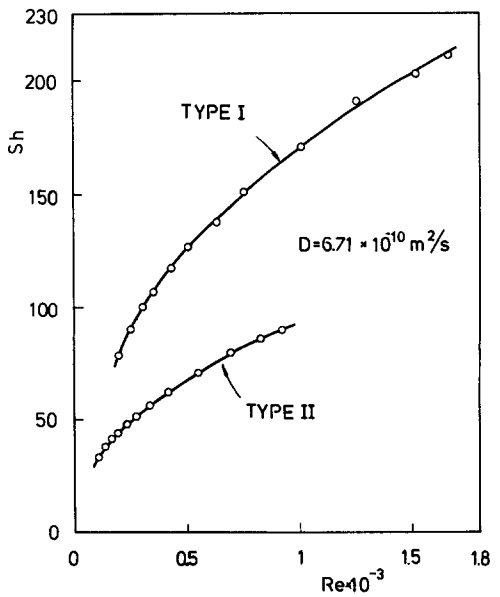

Fig. 7. Dimensionless mean mass transfer coefficient.

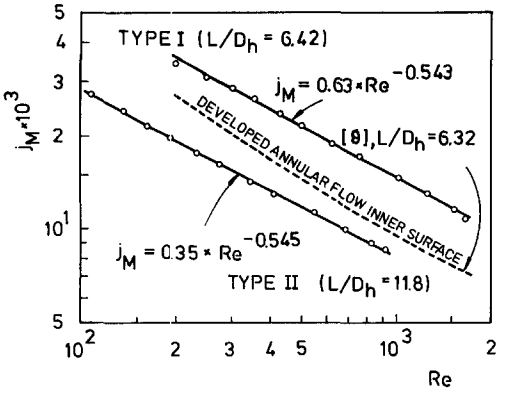

Fig. 8. Mean mass transfer Chilton–Colburn coefficient.

results are shown precisely with the help of correlations

$$j_M = 0.63Re^{-0.543}$$

for the type I model of the rotor (7)

and

$$j_M = 0.35Re^{-0.545} \text{ for the type II model.} \quad (8)$$

The Schmidt number of the electrolyte was known with an accuracy of $\pm 7\%$. The mean square error of the mass transfer Stanton number was equal to 7.4% and for j_M it was equal to 8.8%. The error of the correlations is equal to 17%.

Peculiar features of the cases investigated, such as developing hydraulic boundary layer, comparatively short diffuser-like ducts, non-typical shape of the cross-section of the ducts, curved duct axes and slot-communication of neighbouring ducts, make it difficult to present an appropriate comparison of the results with those of similar investigations because it is difficult to find the latter.

Nevertheless, the results of investigations of the type I model of the rotor can be compared, in Fig. 8, with the results of previous investigations of the author ([9], p. 44, Fig. 6) for the inner surface in a straight annular duct, with $L/D_h = 6.32$ (value almost the same as in the present case), and fully developed flow. The results of present measurements lie higher on the graph, which may be explained firstly by the occurrence of nondeveloped flow at the inlet to the cathode.

Secondly, the intensity of mass/heat transfer may be enhanced thanks to secondary swirling motions in the flow along the duct. The phenomenon [10] occurs under the action of the transversal velocity component w_t of the fluid entering, partially slot-wise, the test section at radial velocity w_r inclined at α to the main stream at the inlet to the duct, as depicted in Fig. 9. Thirdly, the influence of the curved duct axis resulted in inducing a secondary flow due to the centrifugal forces [11, 12], which may also cause an additional enhancement of the mass/heat transfer rate.

The results of measurements were used for simple comparative heat transfer calculations for rotors of type I and II of the same length of 50 mm in an example for dry air at pressure 1 bar and mean temperature of the air of 30°C. Some data for the rotors are given in Table 1. The other main data are given in Table 3.

The latter are the same as for the rotor of the SFE used for flow and heat transfer investigations.†

The calculations based on the Chilton–Colburn analogy between mass and heat transfer:

$$j_M = j_H = St_H\, Pr^{2/3} \quad (9)$$

were made regarding two variants: (1) of equal air flux of 2 N m^3 min^{-1} and (2) of equal Reynolds number of 844, i.e. at Re, which occurred for the rotor of type I at variant 1. It proved for variant 1 that:

$100\%(h_I - h_{II})/h_{II} = 18\%$ and
$100\%[(hA_H)|_{II} - (hA_H)|_I]/(hA_H)|_I = 27\%$.

For variant 2: $h_I \approx 1.05h_{II}$ and
$100\%[(hA_H)|_{II} - (hA_H)|_I]/(hA_H)|_I = 52\%$.

The last value is valid in the whole range of Re common for rotors of both types.

The results allow the type of rotor to be selected from the point of view of intensity of heat transfer. But some comments have to be made.

In the case of entire similarity for straight ducts one correlation $j_M = j_M(Re)$ or $Nu = Nu(Re)$ for all ducts is valid and the mass/heat transfer coefficient is inversely proportional to the hydraulic diameter for the same Reynolds number.

Mass/heat transfer correlations for ducts I and II differ from one another because:

(1) There is no geometric similarity between ducts I and II and therefore there is no similarity of the main flows in them.

(2) Secondary flows are also of different character according to the transversal component of the inflow stream velocity.

In the case of duct I the partially slot-wise inflow of the fluid occurs in the middle regions of the cross-section of the duct, which results in inducing intensive symmetrical secondary flow fields and therefore in the enhancing of the effect of mass/heat transfer.

In the case of duct II the inflow stream is to a great extent tangential to the flat wall of the duct and therefore substantial friction losses in the boundary layer at the flat wall may weaken the secondary flows, resulting in reducing the effects of mass/heat transfer in comparison with duct I.

The curvature ratios of the ducts are $\delta_I > \delta_{II}$, which

† See Acknowledgements.

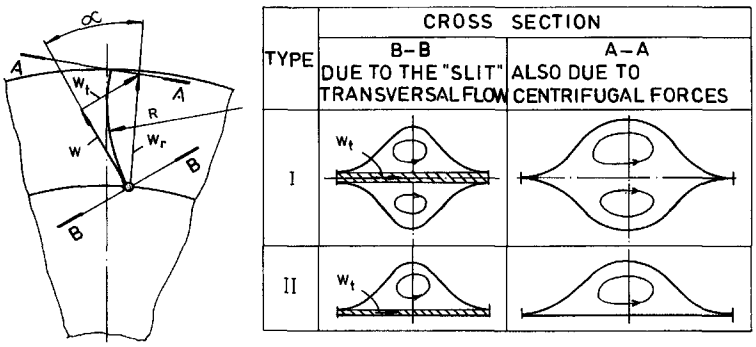

Fig. 9. Secondary flows at inlet and outlet of the curved duct.

Table 3. The other main data for rotors

Dimension	Notation	Units	Rotor of length 50 mm	
			of type I	of type II
Quantity of corrugated elements		pcs	32	26
Quantity of flat elements		pcs	—	27
Overall surface of heat transfer	A_H	m^2	0.319	0.477

causes an intensification of secondary flows in duct I in comparison with duct II [11, 12].

That is why a possibility exists that h_I may even be greater than h_{II}, as given in example above, though $D_{hI} > D_{hII}$, as in this case.

CONCLUSIONS

(1) The usefulness of the electrolytic technique for the experimental investigation of the convective mass/heat transfer coefficient for certain porous structures has been fully confirmed.

(2) The correlations $j_M = j_M(Re)$ for two types of the rotor of the sucking and forcing regenerative heat exchanger for static conditions are presented in a form ready to use.

(3) The technique and form of presentation of the results makes it possible for the optimization to be easily carried out.

Acknowledgements—The work was done within the KBN project No. 905339101 entitled: "Model study on sucking and forcing heat exchanger", which was directed by dr inż. Włodzimierz Wawszczak (Institute of Turbomachinery, Technical University of Łódź, ul. Stefanowskiego 1/15, 90-924 Łódź, Poland), whom the authors wish to thank for the great interest and financial support of the work. The authors would also like to thank mgr inż. Krzysztof Kiedrzyński for assistance in carrying out the experiments.

REFERENCES

1. J. R. de Fries, Rotating heat exchanger of high capacity, Patent U.S.A. No. 3456718 (1969).
2. W. Wawszczak, Fundamental research of sucking and forcing regenerative heat exchanger, *Proceedings of the Eighth Symposium on Heat and Mass Transfer*, pp. 507–516, Polish Academy of Science, Białowieża (1992).
3. T. Mizushina, The electrochemical method in transport phenomena, *Adv. Heat Transfer* **7**, 87–161 (1971).
4. E. R. G. Eckert, *Analogies to Heat Transfer Processes in Measurements in Heat Transfer* (2nd Edn) (Edited by E. R. G. Eckert and R. J. Goldstein). Hemisphere, Washington (1976).
5. M. Hopkowicz and Z. Pietrzyk, Pomiar współczynnika dyfuzji metodą wirującego dysku oraz dynamicznego współczynnika lepkości i gęstości dla układów $K_3Fe(CN)_6$–$K_4Fe(CN)_6$–NaOH, *Inż. Chem.* **VII(4)**, 843–854 (1977) [in Polish].
6. D. M. Lucas, W. A. Davis and B. Gray, Evaluation of local and average convective heat transfer coefficients in a furnace using an electrolytic mass transfer model, *J. Inst. Fuel* 31–37 (1979).
7. J. C. Bazán and A. J. Arvia, The diffusion of ferro- and ferricyanide ions in aqueous solutions of sodium hydroxide, *Electrochimica Acta* **10**, 1025–1032 (1965).
8. M. Eisenberg, C. W. Tobias and C. R. Wilke, Selected physical properties of ternary electrolytes employed in ionic mass transfer studies, *J. Electrochem. Soc.* **103**, 413–416 (1956).
9. B. Bieniasz, Wykorzystanie elektrolizy i analogii między wymianą ciepła i masy w projektowaniu elementów wymienników ciepła z konwekcją wymuszoną, *Wydawnictwo Uczelniane Politechniki Rzeszowskiej im. Ignacego Łukasiewicza*, Rzeszów (1980) [in Polish].
10. W. W. Focke, J. Zachariades and I. Oliver, The effect of the corrugation inclination angle on the thermohydraulic performance of plate heat exchangers, *Int. J. Heat Mass Transfer* **28**, 1469–1479 (1985).
11. Ru Yang and Sung Fa Chang, A numerical study of fully developed laminar flow and heat transfer in a curved pipe with arbitrary curvature ratio, *Int. J. Heat Fluid Flow* **14**, 138–135 (1993).
12. G. J. Hwang and Chung-Hsing Chao, Forced laminar convection in a curved isothermal square duct, *ASME J. Heat Transfer* **113**, 48–55 (1991).